

Optical Engineering

OpticalEngineering.SPIEDigitalLibrary.org

Manufacturing of embedded multimode waveguides by reactive lamination of cyclic olefin polymer and polymethylmethacrylate

Christian Kelb
Raimund Rother
Anne-Katrin Schuler
Moritz Hinkelmann
Maik Rahlves
Oswald Prucker
Claas Müller
Jürgen Rühle
Eduard Reithmeier
Bernhard Roth

SPIE.

Manufacturing of embedded multimode waveguides by reactive lamination of cyclic olefin polymer and polymethylmethacrylate

Christian Kelb,^{a,*} Raimund Rother,^b Anne-Katrin Schuler,^d Moritz Hinkelmann,^a Maik Rahives,^a Oswald Prucker,^d Claas Müller,^b Jürgen Rühle,^d Eduard Reithmeier,^{a,c} and Bernhard Roth^a

^aLeibniz University Hannover, Hannover Centre for Optical Technologies, Nienburger Straße 17, 30167 Hannover, Germany

^bAlbert-Ludwigs-University, Department of Microsystems Engineering—IMTEK, Laboratory for Process Technology, Georges-Köhler-Allee 103, 79110 Freiburg, Germany

^cLeibniz University Hannover, Institute for Measurement and Automatic Control, Nienburger Straße 17, 30167 Hannover, Germany

^dAlbert-Ludwigs-University, Department of Microsystems Engineering—IMTEK, Laboratory for Chemistry and Physics of Interfaces, Georges-Köhler-Allee 103, 79110 Freiburg, Germany

Abstract. We demonstrate the manufacturing of embedded multimode optical waveguides through linking of polymethylmethacrylate (PMMA) foils and cyclic olefin polymer (COP) filaments based on a lamination process. Since the two polymeric materials cannot be fused together through interdiffusion of polymer chains, we utilize a reactive lamination agent based on PMMA copolymers containing photoreactive 2-acryloyloxyanthraquinone units, which allows the creation of monolithic PMMA-COP substrates through C-H insertion reactions across the interface between the two materials. We elucidate the lamination process and evaluate the chemical link between filament and foils by carrying out extraction tests with a custom-built tensile testing machine. We also show attenuation measurements of the manufactured waveguides for different manufacturing parameters. The lamination process is in particular suited for large-scale and low-cost fabrication of board-level devices with optical waveguides or other micro-optical structures, e.g., optofluidic devices. © 2016 Society of Photo-Optical Instrumentation Engineers (SPIE) [DOI: 10.1117/1.OE.55.3.037103]

Keywords: optical sensing; optical waveguides; photonic technologies; reactive lamination.

Paper 151511 received Oct. 29, 2015; accepted for publication Feb. 12, 2016; published online Mar. 8, 2016.

1 Introduction

Polymer optical fibers are key components for a large variety of applications used in daily life such as in-home¹ or automotive² communication networks and illumination applications.³ Especially in consumer electronics, mass-market applications require flexible, reliable, and high-throughput fabrication techniques. To obtain high-throughput fabrication rates, typical processes used such as lamination and hot embossing are most often reel-to-reel compatible. Lamination is especially suited for large-scale production of multilayer systems and has been utilized for the fabrication of different types of optical elements and devices. In addition to the encapsulation of optoelectronic devices such as organic light emitting diodes (OLED)⁴ or integrated circuits in polymer packages,⁵ lamination techniques were also used for high-throughput production of tactile sensors,⁶ gigahertz waveguides,⁷ and optical waveguides.⁸

Current research in integrated optics and photonics focuses on the fabrication of embedded systems in thin polymer foils including waveguides as well as illumination and sensing elements.⁹ Such structures are commonly fabricated by means of hot-embossing processes for microstructuring of substrate layers^{10,11} with the claimed benefit that the processes can be upscaled to a roll-to-roll approach. Usually, to obtain embedded waveguides, a trench is created in a substrate in an initial embossing process. The substrate serves as

cladding and the trench is subsequently filled with a liquid monomer as core material.¹² In a final step, the core material is either cured thermally or by exposure to UV radiation, resulting in a “buried” waveguide structure.

One of the main problems when fabricating optical waveguides by hot-embossing or lamination processes is the chemical compatibility of the core and the cladding materials, which is required to provide long-term stability of the photonic system. Bonding of core and cladding most often relies on interdiffusion of polymer chains at the boundary between the two materials, initiated by heat and pressure during the lamination or hot-embossing process.¹³

A suitable combination of core and cladding materials for waveguide production, therefore, depends on their optical, mechanical, and thermal properties. For instance, to enable light guiding inside the waveguide, the refractive index of the core needs to be higher than the refractive index of the cladding (or substrate).¹⁴ In addition, the mechanical and thermal properties of the substrate and the core materials have to meet the requirements of the hot-embossing or lamination process such that geometrical deformations of relevant optical structures due to the fabrication process are negligible. Polymers used in lamination and hot-embossing processes are thermoplastics, which are deformable at temperatures above their glass transition temperature (T_g). Hence, processing core and cladding above the glass transition temperatures of both materials leads to a deformation induced by

*Address all correspondence to: Christian Kelb, E-mail: christian.kelb@hot.uni-hannover.de

pressure and heat during the hot-embossing or lamination process. As a consequence, the optical quality of the waveguide may be decreased and propagation losses become comparably high.

In this work, we present a lamination process to create embedded multimode (MM) waveguides integrated in thin polymer foils by means of a reel-to-reel lamination technique. Due to the low scattering, good availability, cost-effectiveness, and suitable refractive indices, we chose polymethylmethacrylate (PMMA) with a refractive index of 1.49 and cyclic olefin polymer (COP) with a refractive index of 1.53 as substrate and core material, respectively.

While the material attenuation of the core material chosen is rather high for long-distance waveguides and even not optimal for in-house communication (about 1.23 dB/cm¹⁵), the resulting attenuation is certainly suitable for the large-scale production of board-level devices. Such devices, e.g., lab-on-a-chip or optofluidic devices, rely on relatively short optical connections of a few centimeters length. Also they profit most from a cost-effective production process as they are usually discarded after one use due to contamination from the analyte.

Both polymers are, in principle, not chemically compatible, which would lead to a delamination of core and cladding under stress. We demonstrate here, for the first time to our knowledge, that utilizing a reactive lamination agent based on PMMA copolymers containing photoreactive 2-acryloyloxyanthraquinone (PMMA-*co*-AOAQ) repeat units, which has been presented previously¹⁶ in a more general context, leads to mechanically stable, functioning waveguides with a high process repeatability which could allow low-cost and large-scale production of embedded waveguides using commercially available polymers. We present results from optical characterization measurements and delamination tests to investigate the performance and mechanical stability of the fabricated waveguides.

2 Waveguide Materials and Fabrication

To enable a large-scale and low-cost reel-to-reel process to fabricate embedded waveguides, we employed a lamination process where the core polymer is deployed as filament with a circular cross-section and a diameter of 100 μm . The filament is fed between a sub- and a superstrate layer made from a cladding polymer material, which get thermally fused together during the lamination process. The filament becomes chemically connected to the substrate after a brief UV treatment. For our waveguide fabrication process, we chose the COP Zeonex 480R as core material and two different PMMA types as sub- and superstrate material. Note that our process is not limited to a circular geometry of the waveguide core, but could, in principle, also be applied to non-circular geometries.

Table 1 shows the refractive index n and the glass transition temperature T_g of both materials. The used PMMA and COP exhibit a refractive index difference of $\Delta n = n_{\text{PMMA}} - n_{\text{COP}} = 0.035$, and the difference in the glass transition temperatures accounts for $\Delta T_g = 25^\circ\text{C}$. In terms of waveguide fabrication, the difference ΔT_g is an important parameter for the presented process since the T_g of the core material needs to be sufficiently high to withstand the thermal load during the lamination process without suffering core deformation. At the same time, the T_g of the

Table 1 Glass transition temperatures and refractive indices of the core-cladding material combination used for waveguide applications^{15,17}

Material	T_g ($^\circ\text{C}$)	n (@ 589 nm)
Plexiglas 99524 GT	113	1.49
Zeonex 480R	138	1.525

cladding material needs to be sufficiently low to obtain a uniform bond between sub- and superstrate at a given lamination temperature. This is fulfilled by the materials given in Table 1, other suitable material combinations can be found, e.g., in Ref. 18.

To form a mechanically stable waveguide, we need to achieve a permanent bond between the COP core and the PMMA cladding material. For this, we first investigated the bond quality obtained by standard lamination. We observed that PMMA and COP foils do not form a monolithic block during standard lamination and can easily be delaminated manually as both are immiscible and no interdiffusion of polymer chains occurs. As a result, the manufactured samples were mechanically unstable and not resistant toward, e.g., external mechanical loads or intrusion of environmental humidity between the laminated layers.

However, lamination of COP and PMMA polymers using a reactive lamination agent based on PMMA copolymers containing 2-acryloyloxyanthraquinone (AOAQ) moieties, which are incorporated in the polymer backbone, was demonstrated¹⁶ recently. There, the “glue” layer was coated onto the COP substrate and activated through UV-irradiation. The AOAQ moiety of the copolymer, which acts as a reactive agent, can be activated by irradiation of UV light with wavelengths of either 250 or 365 nm. Consequently, the activated agent inserts into aliphatic CH-bonds of the COP film, building a covalent connection between the COP and the attached PMMA layer.¹⁶ Additionally, COP and PMMA are chemically rather different and, therefore, are immiscible, which is why a diffusion of the PMMA-based reactive lamination agent into the COP core material can be excluded. Since the authors reported satisfactory success on bonding these two materials, we adapted the reactive lamination agent to the roll-to-roll production of embedded waveguides.

For waveguide fabrication, the reactive agent is applied onto the COP filaments by spray coating utilizing a Walter Pilot[®] Signier airbrush mounted on a modified CNC router. This procedure ensures a uniform distribution of the lamination agent on the filaments. The filaments are rotated three times around their optical axes to enable a homogeneous coating of the entire surface of the core filaments as shown in Fig. 1. The filaments were fixed in an acrylic frame under slight tension during the coating process. The total length of the coated filaments was ~ 200 mm. During coating, marginal oscillations of the filaments were observed, depending on the distance between the filaments and the airbrush nozzle. The filament movement was induced by the airflow from the nozzle and weakened with increasing distance between filaments and nozzle. We did not evaluate the impact of the oscillations on the coating quality which, however, will be necessary for a reliable mass-production process.

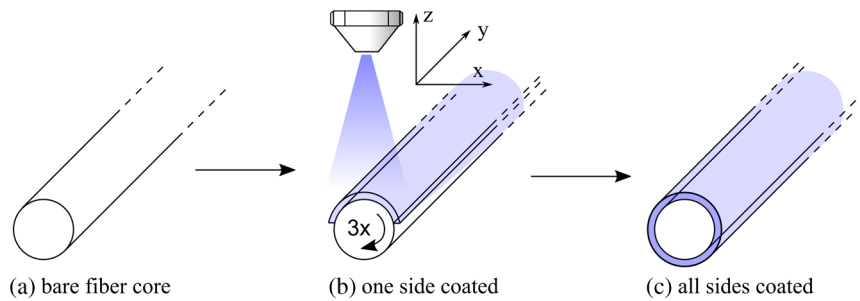


Fig. 1 Schematic of the coating process; (a) bare fiber fixed in acrylic frame (not shown), (b) coating from one side by moving the airbrush along the filament's length, (c) after three rotations, the filament is coated from all sides.

Note that the coating technique can be upscaled to a roll-to-roll process with three nozzles arranged in a circular fashion around a moving filament that is spooled through the nozzle arrangement and, thus, coated uniformly. Of course, other technologies such as dip-coating would also be possible, although with the disadvantage of a significantly increased solvent exposure of the coated filament. In this work we tried to keep solvent exposure to a minimum and we chose spray coating as the deposition method for the reactive agent.

Thickness measurements were conducted with a confocal microscope on samples that were sprayed on a silicon wafer. The thickness of the coating was then read out by evaluation of the distance of the two peaks in the resulting confocal curve and was found to be in the order of $0.9 \mu\text{m}$. Since the filaments were coated using the same parameters, we estimate the thickness of the coating to be in the same range.

To investigate the bond quality of COP on different PMMA substrates, we prepared samples consisting of a Zeonex 480R filament and PMMA 99524 GT as well as PMMA 0F058 substrates, respectively. The two types of PMMA differ mainly in the attenuation of UV light, the latter showing 90% transmittance for UV light¹⁹ (280 to 380 nm) compared to 12.2% transmittance of the PMMA 99524 GT substrate.¹⁷ Each COP-PMMA configuration was prepared with and without reactive lamination agent to investigate the feasibility of the reactive lamination process utilizing commercially available PMMA types, which commonly contain varying amounts of UV stabilizers.

The experimental setup which was utilized for the lamination process is shown in Fig. 2. The lamination was carried out using an Ozatec hot roll laminator (HRL) 350 HRL, with adjustable pressure p , feed rate v_f , and gap width g between the laminator drums. These parameters were kept constant during each lamination run and are given in Table 2. The sample components consisting of substrate, filament, and

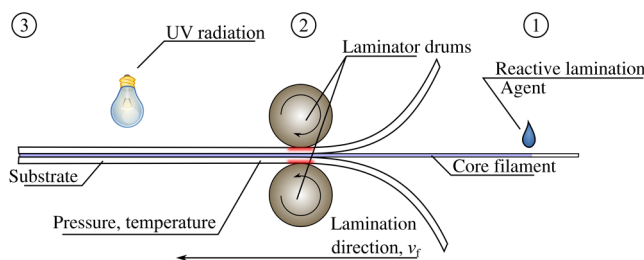


Fig. 2 Schematic of the (1) coating, (2) lamination, and (3) irradiation processes.

Table 2 Lamination parameters used for the process described in Fig. 2.

Pressure	$p = 1 \text{ Bar}$
Feedrate	$v_f = 0.3 \text{ m/min}$
Gap width	$g = 0 \text{ mm}$

superstrate were aligned manually before lamination. The size of the fabricated samples was $\sim 30 \text{ mm} \times 20 \text{ mm}$. For the extraction tests, the filament was aligned parallel to the shorter edge of the sample and protrudes from the laminated substrate layers by at least 50 mm.

With a gap width of 0 mm between the lamination drums, the thickness of the laminated system is solely dependent on the pressure applied. For a gap width greater than zero, the resulting thickness would also be reduced with increasing pressure, but it would be limited at the lower end by the set gap width.

After filament alignment, lamination runs were carried out at two lamination temperatures. For different substrate materials, we used the lamination temperatures and substrate materials given in Tables 2 and 3. Note that we used commercially available substrate materials with different thicknesses as provided by the manufacturer (Evonik).

Note that the lamination temperature describes the temperature of the laminator drums and is not equal to the core temperature of the samples during lamination. The core temperature is lower and depends on several parameters such as drum temperature, lamination speed, substrate thickness, and thermal conductivity of the substrate material. The lamination temperature was chosen by conducting a series of manual peel-off tests while increasing the temperature with every sample. As soon as the substrate passed the peel-off

Table 3 Lamination temperatures for different substrate materials and thicknesses.

Substrate Material	Thickness (μm)	Lamination Temperature T_L ($^\circ\text{C}$)
PMMA 99524 GT	175	145
PMMA 0F058	200	145
PMMA 0F058	200	165

test (i.e., no delamination occurred), we did not raise the lamination temperature further to prevent unnecessary deformation of the core filament.

After the lamination process, the samples were irradiated by UV light with a center wavelength of $\lambda = 254$ nm to trigger the AOAQ-initiated reactive lamination of filament and substrate. The UV radiation dose was adjusted according to the employed substrate material and accounts for 10.8 and 1 J/cm² in the case of PMMA 99524 GT/Zeonex 480R and PMMA 0F058/Zeonex 480R material combinations, respectively. The exposure dose for the PMMA 99524 GT substrate material was chosen higher compared to the one for PMMA 0F058 to account for the decreased UV transmittance due to the higher contents of UV stabilizers.

3 Experimental Setup and Method for Optical and Mechanical Analysis

To quantify the performance of the produced waveguides, two main aspects need to be addressed: first, the waveguides need to be stable under mechanical loads and, second, propagation losses inside the waveguide need to be reasonably low.

3.1 Setup for Mechanical Characterization

Mechanical stability of the embedded waveguides was determined by extraction tests using a custom build precision tensile testing machine as shown in Fig 3(c). The tensile testing machine consists of two sledges guided on air-bearings to minimize breakaway forces, a force sensor and a stepper drive. The sample was mounted between the two sledges and fixated on the substrate side by a clamp while the filament which sticks out of the substrate sample was clamped between two rubber plates to minimize notch effects.

The right, larger sledge is movable and connected to the stepper drive with a spindle, the left, smaller sledge can move only inside the clearance of its connection to the force sensor. The intended position of the substrate and filament is sketched in the photograph in Fig. 3(c).

Prior to the extraction tests, no initial strain was applied to the free filament of the sample and the force sensor output was leveled to the zero position. To evaluate the mechanical behavior of each waveguide sample, strain measurements were carried out by constantly increasing the distance between the sledges, while monitoring the load on the waveguiding filament.

3.2 Setup for Optical Characterization

To determine the propagation losses inside the laminated waveguides, the optical characterization of the waveguide

structures was carried out using the cutback interrogation method.²⁰ For attenuation measurements, we utilized the setup as shown in Fig. 4, which consists of a sample holder, a 50- μ m MM glass-optical fiber, and an Ophir Spiricon[®] 620U beam profiler equipped with a 20 \times Olympus[®] Plan N microscope objective. Attenuation is measured by launching incoherent light from a Thorlabs[®] M625F1 fiber-coupled LED at a center wavelength of $\lambda = 625$ nm into the entrance facet of the waveguide using the MM fiber. We monitored the intensity of the light which is emitted from the other facet by calculating the intensity sum over all image pixels as displayed by the beam profiler in a certain region of interest (ROI). With the known length l of the waveguide and by cutting the waveguide back in several steps (in this case six to seven steps), we were able to measure the relative output power that was exponentially increasing for a smaller l .

To minimize potential sources of errors for our experiments, we only cut back the facet that was monitored by the beam profiler, leaving the other facet unchanged. We also used the live display of integrated counts inside the ROI of the beam profiler as depicted in Fig. 4 to account for the best coupling every time the waveguide was cut back and had to be placed again in our setup. We held the sample fixed while we used two XYZ-translational stages to position the illumination fiber and the beam profiler, respectively. This experiment was carried out for both sub- and superstrate materials as well as for the increased lamination temperature for the PMMA 0F058 substrate.

Figure 3(a) shows the clamped substrate with embedded filament in the optical test setup. Light is coupled into the waveguide from the upper left side while the other waveguide facet on the lower right side was monitored. The illuminated waveguide is shown in Fig. 3(b).

4 Results and Discussion

4.1 Analysis of Mechanical Properties

The analysis of the mechanical properties of the laminated polymer structures was performed using the tensile testing machine as shown in Sec. 3. Figure 5(a) shows the force over travel for an extraction test of coated filament and Fig. 5(b) of an uncoated filament for the PMMA 0F058 substrate. For the uncoated filament, a sawtooth progress of the force was observed while the filament was extracted from the two laminated substrate layers, indicating a stick-slip effect until the filament was removed completely at a displacement of ~ 8 mm. For the coated filament, a linear increase in force over the first 0.5 mm shows the elastic deformation of the filament, followed by a decreased force gradient over travel

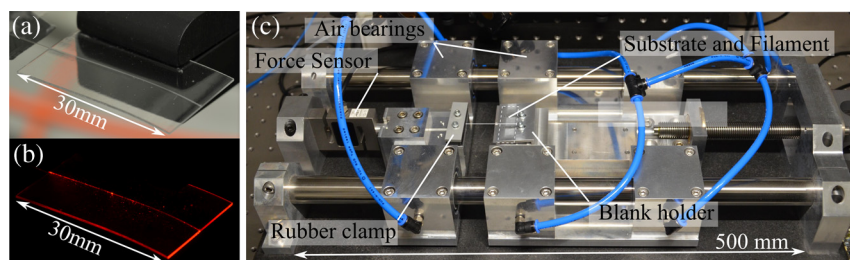


Fig. 3 Image of the laminated filament: (a) under ambient light; (b) red incoherent light coupled into the waveguide; (c) image of the tensile testing machine used to characterize the mechanical bond.

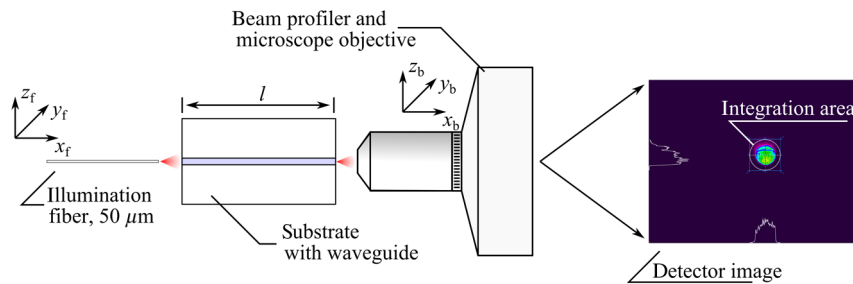


Fig. 4 Schematic of the experimental setup used for attenuation measurements. The substrate and waveguide is held with a clamp and illuminated with a 50- μm MM fiber from one side. The other waveguide facet is monitored with a beam profiler and its output image is integrated in a ROI to compute a relative intensity.

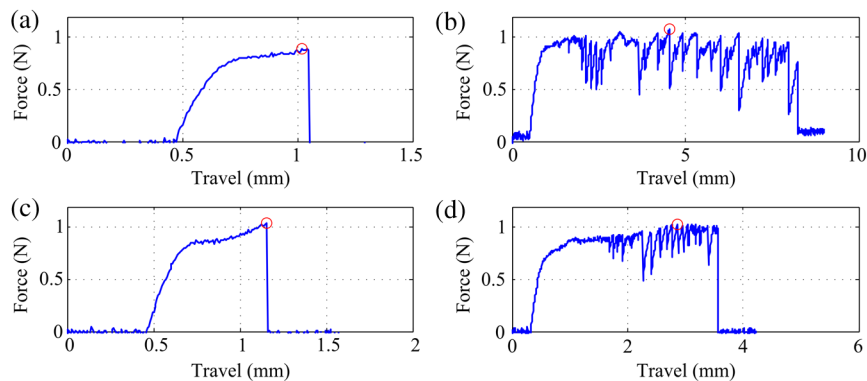


Fig. 5 Force over travel for (a) coated and (b) uncoated filament with substrate material PMMA 0F058. Force over travel for (c) coated and (d) uncoated filament with substrate material PMMA 99524 GT. The red circle marks the maximum force, respectively.

caused by necking of the filament. At a displacement of 1.1 mm, the filament tore.

Comparing both force progressions, we observed that the coated filament tore at a slightly lower force compared to the uncoated filament. A thorough investigation showed an average tear force for the coated filaments of 0.945 N with a standard deviation of 0.062 N over six measurements. The maximum force for the uncoated filament was 0.994 N with a standard deviation of 0.054 N over three measurements. The difference in maximum forces can be explained with a certain notch effect on the coated filaments, as they were monolithically bonded to the substrate material, while the uncoated filaments were friction-locked between sub- and superstrate and, therefore, suffered no notch effect.

Figure 5(c) shows the force progression of an extraction test for PMMA 99524 GT as substrate material for the coated filament and Fig. 5(d) for uncoated filament. Again, a stick-slip effect can be observed for the uncoated case while the filament tears without any sign of slipping for the coated filament at a travel of 1.2 mm. Although this depicted case shows a result where the tear force in the coated case is as high as the maximum force in the uncoated case, the statistical evaluation of all experiments shows an average tear force of 0.936 N with a standard deviation of 0.098 N for coated filaments (again over six measurements) and an average maximum extraction force of 1.096 N with a standard deviation of 0.099 N for uncoated filaments (over three measurements).

Our measurements on all manufactured samples can be summarized as follows: all samples without reactive lamination agent showed a sawtooth-like behavior of force over

travel. Additionally, for almost all of the uncoated samples, the filament could be removed completely from the laminated sub- and superstrate bulk. In contrast, all coated samples with a reactive lamination agent did not show a stick-slip behavior upon force application. In each case, the filaments tore after a maximum force was reached.

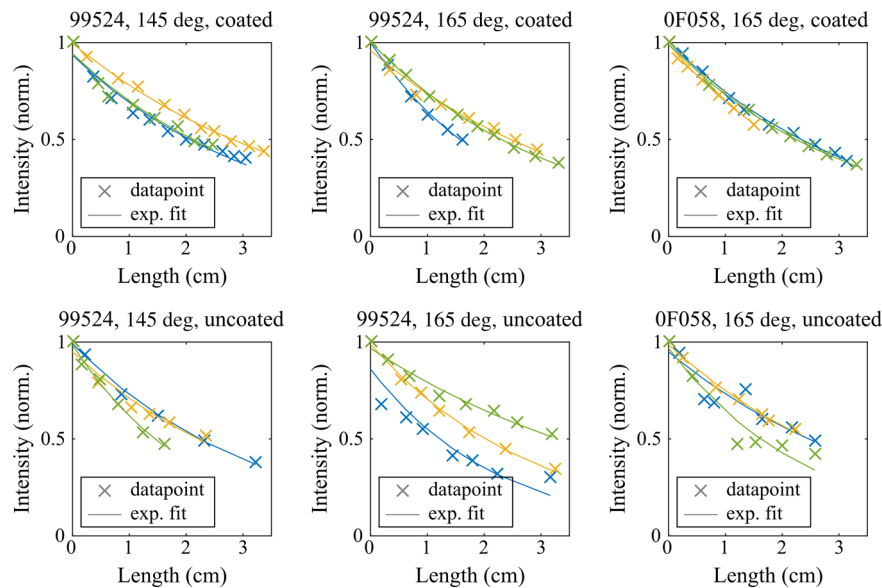
Using an optical microscope and imaging the front surface of the embedded waveguide, we also found that the COP core was circular after lamination with drum temperatures of 145 °C. Only the samples produced with a lamination temperature of 165 °C showed a core that was slightly elliptical, with the short axis measuring 85 μm and the long axis 116 μm . In addition to the raised core temperature, this effect could also be amplified by the stiffer substrate material PMMA 0F058 for which the increased lamination temperature was required.

4.2 Measurement of Optical Attenuation

The results of the optical characterization are shown in Table 4 and, graphically, in Fig. 6. The measurements were carried out once for each sample as the cut-back method leads to a destruction of the sample. For the samples fabricated with and without reactive PMMA-co-AOAQ coating, respectively, we obtained similar values for propagation losses between 1.23 to 1.54 dB/cm. No significant difference in attenuation between the two types of structures was observed. For each set of parameters, one sample with a total length of 15 cm was produced and later cleaved into three parts with equal length, resulting in 18 samples in total.

Table 4 Measured attenuation of manufactured waveguide samples for both substrate materials utilized and different lamination temperatures. The standard deviation is given in brackets.

Sub- and superstrate material and T_L	Attenuation @ 625 nm without coating	Attenuation @ 625 nm with coating
PMMA 99524 GT, $T_L = 145^\circ\text{C}$	1.54 dB/cm (0.424 dB/cm)	1.23 dB/cm (0.141 dB/cm)
PMMA 99524 GT, $T_L = 165^\circ\text{C}$	1.43 dB/cm (0.540 dB/cm)	1.45 dB/cm (0.404 dB/cm)
PMMA 0F058, $T_L = 165^\circ\text{C}$	1.37 dB/cm (0.351 dB/cm)	1.39 dB/cm (0.139 dB/cm)

**Fig. 6** Results of the optical attenuation measurements using the cut-back method. First row: coated samples. Second row: uncoated samples. Three samples per parameter combination were used. Sample type, lamination temperature T_L , and coating information are given on top of each panel, respectively. The color coding indicates the different samples studied. Note the higher variance of the data points in the uncoated case.

Although the attenuation of the measured waveguides does not show a clear increase or decrease between coated and uncoated specimens, the deviation of the attenuation between the samples of each parameter set was significantly lower in the case of the coated filaments. Also, the difference between the exponential fit function and the data points is smaller in the case of the coated samples, indicating more constant cleaving results. We attribute this effect to the better mechanical stability of the samples with lamination agent which results in a more controlled process of production as well as the later cleaving for characterization.

5 Conclusions

In this work, we demonstrated the successful fabrication of embedded waveguides utilizing PMMA and COP polymers as cladding and core material, respectively, by means of a reactive lamination agent. During UV activation, the reactive lamination agent PMMA-co-AOAQ builds chemical bonds between the otherwise chemically incompatible materials and, thus, enables the lamination of core and cladding materials. Lamination results were characterized with respect to their mechanical and optical properties. A series of delamination tests using a high-precision tensile testing machine were carried out to quantify the mechanical stability of the

produced waveguides. The results of the extraction tests showed a distinct stick-slip effect when extracting the core filament from the PMMA substrate laminated with a standard process, i.e., without a lamination agent. In contrast, the coated core filament after reactive lamination tore before reaching a displacement exceeding its tensile elongation. Furthermore, the reduced tear force for the coated filaments indicates a notch effect that can, in principle, only occur for monolithic and, thus, uniform, strong, and durable links between filament and sub- and superstrate.

In addition, we carried out optical propagation loss measurements of the fabricated waveguide structures. The results indicate that there is no significant difference in propagation loss when using the reactive lamination agent compared to the uncoated samples. However, the deviation of the attenuation results as well as the error between the fit functions and the data points is smaller in the coated case, indicating a more stable system and, thus, more reliable waveguides. This is fundamental for the production of, e.g., optofluidic devices that are produced in large quantities and cannot be calibrated individually before use. Hence, the reactive lamination agent is suitable for efficient lamination of waveguide structures which appear suited for the realization of integrated optical sensor systems in future. The process

enables large-scale and low-cost fabrication of such structures and may ultimately lead to production techniques for micro-optical or lab-on-a-chip devices.

In a next step, we also plan to utilize the process for the realization of all-polymer optical displacement sensors based on the systems developed earlier⁹ and to further investigate the feasibility of the reactive lamination process for production of more complex optical devices. This will also include a series of tests to quantify the influence of environmental parameters, including temperature cycling and long-term exposure to UV radiation.

Acknowledgments

We acknowledge funding by the German Research Foundation within the Collaborative Research Center SFB/TRR 123—Planar Optronics Systems (PlanOS).

References

1. S. Ten, "In-home networking using optical fiber," in *2012 Optical Fiber Communication Conf. and Exposition and the National Fiber Optic Engineers Conf. (OFC/NFOEC 2012)*, Los Angeles, CA (2012).
2. Y. Tsukamoto, "Plastic optical fiber (POF) technology for automotive, home network systems," in *IEEE 802.1/802.3 Joint Interim Meeting*, Norfolk, VA (2014).
3. I. Ullah and S. Shin, "Highly concentrated optical fiber-based daylighting systems for multi-floor office buildings," *Energy Build.* **72**, 246–261 (2014).
4. M. H. Park et al., "Flexible lamination encapsulation," *Adv. Mater.* **27**(29), 4308–4314 (2015).
5. V. Iyer et al., "Encapsulation of integrated circuits in plastic microfluidic systems using hot embossing," in *2015 Transducers—2015 18th Int. Conf. on Solid-State Sensors, Actuators and Microsystems, Anchorage, Alaska*, pp. 1822–1825 (2015).
6. H. P. Phan et al., "Graphite-on-paper based tactile sensors using plastic laminating technique," in *28th IEEE Int. Conf. on Micro Electro Mechanical Systems (MEMS 2015)*, pp. 825–828 (2015).
7. H. Uchimura, T. Takenoshita, and M. Fujii, "Development of the 'laminated waveguide'," in *1998 IEEE MTT-S Int. Microwave Symp. Digest*, pp. 1811–1814 (1998).
8. S. Kopetz, E. Rabe, and A. Neyer, "High-temperature stable flexible polymer waveguide laminates," *Electron. Lett.* **42**(11), 634 (2006).
9. C. Kelb et al., "Realization and performance of an all-polymer optical planar deformation sensor," *IEEE Sensors J.* **15**(11), 7029–7035 (2015).
10. M. Rahlves et al., "Flexible, fast, and low-cost production process for polymer based diffractive optics," *Opt. Express* **23**(3), 3614 (2015).
11. L. Peng et al., "Micro hot embossing of thermoplastic polymers: a review," *J. Micromech. Microeng.* **24**(1), 13001 (2014).
12. A. Günther et al., "Cladded self-written multimode step-index waveguides using a one-polymer approach," *Opt. Lett.* **40**(8), 1830–1833 (2015).
13. C. Bonten, *Kunststofftechnik: Einführung und Grundlagen*, Hanser, Carl, München (2014).
14. J. Jahns, *Photonik: Grundlagen, Komponenten und Systeme*, Oldenbourg, München (2001).
15. D. Takahashi, *Cyclo Olefin Polymer (COP): Zeonex*, Zeon Corporation, Japan (2012).
16. A. K. Schuler et al., "A novel reactive lamination process for the generation of functional multilayer foils for optical applications," *Procedia Technol.* **15**, 147–155 (2014).
17. "Technical information: Plexiglas film 99524," Evonik Performance Materials GmbH, Darmstadt, Germany, (2015).
18. S. Bäumer, *Handbook of Plastic Optics*, 1st ed., Wiley-VCH, Weinheim, Great Britain (2005).
19. "Technical information: Plexiglas film 0F058," Evonik Performance Materials GmbH, Darmstadt, Germany, (2015).
20. D. B. Keck and R. Tynes, "Spectral response of low-loss optical waveguides," *Appl. Opt.* **11**(7), 1502–1506 (1972).

Christian Kelb received his diploma degree in mechanical engineering in 2011 from Leibniz University Hannover. He is currently pursuing his PhD in engineering at the Hannover Centre for Optical Technologies (HOT) of the Leibniz University Hannover. His main interests are in the field of optical technologies, in particular optical sensing and manufacturing by means of lamination, hot embossing, and injection molding.

Raimund Rother received his diploma degree in chemistry in 2012 from Albert-Ludwigs-University Freiburg. Since 2013, he has been working on the development of the reactive lamination process as a PhD student in the Laboratory for Process Technology, Department of Microsystems Engineering (IMTEK) at Albert-Ludwigs-University of Freiburg.

Anne-Katrin Schuler received her diploma degree in chemistry with focus on macromolecular chemistry in 2012 from Albert-Ludwigs-University Freiburg. Since 2012 she has been a PhD student at the Department of Microsystems Engineering (IMTEK), Laboratory for Chemistry and Physics of Interfaces at the University of Freiburg, working on the development of reactive polymer systems for the reactive lamination process.

Moritz Hinkelmann is a student in the optical technologies master course of Leibniz University Hannover. He is currently pursuing a student project at the HOT.

Maik Rahlves graduated in physics at the University Oldenburg in 2006. From 2006 to 2009, he was a research associate at the Institute of Measurement and Automatic Control, University Hannover, focusing on confocal microscopy, interferometry, and surface metrology. Since 2009 he has been with the Hannover Centre for Optical Technologies, University Hannover. He received his PhD in mechanical engineering in 2011. Since then he has headed the applied optics group with interests in optical metrology, holography, and polymer micro-optics.

Oswald Prucker studied chemistry at the University Bayreuth, where he received his PhD in 1995. The work was supervised by Jürgen Rühle. He then was with Prof. Curtis W. Frank at the Chemical Engineering Department, Stanford University, as a postdoctoral fellow. In 1998, he again joined the Rühle group at the Max-Planck-Institute for Polymer Research in Mainz. Now he is senior scientist in Jürgen Rühle's group at the Department of Microsystems Engineering (IMTEK), University Freiburg.

Claas Müller studied physics from 1986–1991 at the University Karlsruhe. Following the physics diploma, he earned his PhD in 1994 at Forschungszentrum Karlsruhe, Institute for Micro Structure Technology, working on miniaturized spectrometer systems, fabricated by LIGA technology. Since 1996, he has been a graduate council at the Chair of Process Technology of the Department of Microsystems Engineering (IMTEK). In 1999, he was appointed substitutional manager, and in 2004, managing director of the Chair of Process Technology.

Jürgen Rühle studied chemistry at the Universities Münster and Mainz. In 1989 he received his PhD in Mainz. After a postdoctoral stay at IBM, California, he returned to Germany in 1991. In 1995, he completed his Habilitation at University Bayreuth and joined the MPI of Polymer Research, Mainz, as associate professor. In 1999, he became full professor and Chair for Chemistry and Physics of Interfaces at the Department of Microsystems Engineering (IMTEK), University Freiburg.

Eduard Reithmeier received his diploma in mechanical engineering in 1977 and his diploma in mathematics in 1979 from Technical University Munich. In 1989, he received his PhD in mechanical engineering from the same university. From 1992 to 1996, he was technical director of the business divisions automation and medical engineering at the Bodenseewerk Gerätetechnik GmbH in Ueberlingen. Since 1996 he has been professor of mechanical engineering and director of the Institute for Measurement and Control, University Hannover.

Bernhard Roth obtained his PhD in 2001 at University Bielefeld. From 2002 to 2007, he was group leader at University Duesseldorf and obtained his Habilitation in quantum optics in 2007. From 2007 to 2010, he was associate professor at University Duesseldorf and from 2011 to 2012 managing director at the research center innoFSPEC, University Potsdam and Leibniz Institute for Astrophysics Potsdam. Since 2012 he has been director of the Hannover Centre for Optical Technologies and since 2014 professor at the University Hannover.